Original Article

Taiwan J Ophthalmol 2023;13: 505-519

Access this article online

Quick Response Code:

Website: http://journals.lww.com/TJOP

DOI: 10.4103/tjo.TJO-D-23-00134

Clinical and diagnostic imaging profile of three anterior segment dysgenesis disorders presenting with infantile corneal opacities

Ananya Kaginalkar[1], Radhika Tandon[1]*, M. Vanathi[1], Noopur Gupta[1], Viney Gupta[1], Seema Sen[1], Seema Kashyap[1], Arundhati Sharma[2]

Abstract:

PURPOSE: To describe three anterior segment dysgenesis disorders with infantile corneal opacities, namely, congenital hereditary endothelial dystrophy (CHED), primary congenital glaucoma (PCG), and Peters anomaly (PA) in terms of clinical characteristics, histopathology, genetic association, and diagnostic imaging profiles using imaging modalities such as ultrasound biomicroscopy (UBM) and microscope-integrated intraoperative optical coherence tomography (i-OCT).

MATERIALS AND METHODS: Seventy-four eyes with 22 eyes of CHED, 28 eyes of PA, and 24 eyes of PCG were clinically evaluated and underwent imaging using UBM and i-OCT. Corneal buttons of 16 operated patients underwent histopathological analysis, while genetic analysis was done in 23 patients using whole-exome sequencing.

RESULTS: Corneal diameters (CD) and UBM parameters like anterior chamber depth (ACD), iris thickness (IT), and ciliary body (CB) thickness revealed a statistically significant difference between the three categories. In PA, 9 eyes had a third rare phenotype with only a posterior corneal defect with no iris adhesions. Genetic mutations were seen in all tested patients with CHED, in 83.3% of patients with PCG, and in 80% of patients with the third type of PA. i-OCT helped in the characterization of corneal opacity, identification of posterior corneal defects, iridocorneal adhesions, and contour of Descemet's membrane.

CONCLUSION: Overlapping phenotypes of the above disorders cause a diagnostic dilemma and parameters like CDs, UBM ACD, IT, and CB thickness help differentiate between them. i-OCT can help in classifying the diseases in a high resolution, non-contact manner, and can better delineate corneal characteristics. The rare third type of PA phenotype may have a genetic association.

Keywords:

Anterior segment dysgenesis, congenital hereditary endothelial dystrophy, intraoperative optical coherence tomography, primary congenital glaucoma, Type 3 Peters anomaly, ultrasound biomicroscopy

[1]Dr. RP Center for Ophthalmic Sciences, All India Institute of Medical Sciences, [2]Department of Anatomy, All India Institute of Medical Sciences, New Delhi, India

***Address for correspondence:**
Prof. Radhika Tandon, Dr. RP Center for Ophthalmic Sciences, All India Institute of Medical Sciences, Ansari Nagar, New Delhi - 110 029, India.
E-mail: radhika_tan@yahoo.com

Submission: 07-09-2023
Accepted: 09-10-2023
Published: 20-12-2023

Introduction

Anterior segment dysgenesis (ASD) refers to developmental disorders of the anterior segment that occur due to the arrest of neural crest cell migration and differentiation and includes a broad umbrella of disorders.[1-3] Congenital corneal opacities (CCO) are reported to occur in approximately 6:1,00,000 newborns if congenital glaucoma is included. ASD is an important cause of CCO.[4] ASD disorders presenting characteristically with corneal opacities that develop in infancy are congenital hereditary endothelial dystrophy (CHED), primary congenital glaucoma (PCG), Peters anomaly (PA), sclerocornea, and aniridia.[3]

How to cite this article: Kaginalkar A, Tandon R, Vanathi M, Gupta N, Gupta V, Sen S, *et al*. Clinical and diagnostic imaging profile of three anterior segment dysgenesis disorders presenting with infantile corneal opacities. Taiwan J Ophthalmol 2023;13:505-19.

About 50% of patients with ASD disorders develop glaucoma. Studies demonstrating the coexistence of congenital glaucoma with CHED and PA highlight that these conditions do present with overlapping features. Thus, ASD disorders occur due to a complex interplay of developmental, embryological, and genetic factors, often presenting in the form of phenotypic overlaps, and pose to be diagnostic clinical challenges.[5]

This study aims to highlight the clinical features and to characterize these overlapping ASD disorders, namely, CHED, PCG, and PA using imaging modalities, in order to guide their accurate diagnosis. It is imperative that an ophthalmologist must make an accurate diagnosis of these disorders to predict the natural history of the disorder, to search for associated ocular and systemic abnormalities, to provide genetic counseling to the parents of children with these disorders, to begin appropriate medical or surgical therapy promptly for these patients, and to anticipate the course of visual prognosis.[6]

Materials and Methods

Patient recruitment and study design

This study was an observational ambispective study. The patients were recruited for a period of 1.5 years from October 30, 2020, to January 30, 2022 from Dr. Rajendra Prasad Center for Ophthalmic Sciences, All India Institute of Medical Sciences, New Delhi, after due ethical clearance from the institutional review board (Institutional Review Board name: Ethics Committee AIIMS, Approval number: IEC PG-199/24.06.2020, RT-23/26.08.2020). Written informed consent was obtained from the adult patients and from parents/guardians of children in the study. A total of 42 patients (74 eyes) with 11 patients diagnosed with CHED (22 eyes), 18 patients diagnosed with PA (28 eyes), and 13 patients diagnosed with PCG (24 eyes) were recruited. Clinical and imaging details of six patients were obtained from old surgical records (retrospective), while clinical and imaging details of 36 patients were obtained prospectively.

Inclusion and exclusion criteria

Patients of any age group diagnosed with ASD with corneal opacities that had developed within 1 year of age and meeting the standardized clinical diagnostic criteria for either CHED, PCG, and PA were included. The diagnosis was confirmed by two cornea consultants and one glaucoma consultant, each having more than 10 years of experience in their respective subspecialties.

Patients with corneal opacities due to sclerocornea, aniridia, Axenfeld–Rieger anomaly, posterior polymorphous corneal dystrophy (PPCD), iridocorneal endothelial (ICE) syndrome, corneal opacities due to undetermined causes, as well as patients with positive TORCH (Toxoplasma, Rubella, Cytomegalovirus, Herpes Simplex, HIV) test, metabolic disorders, history of birth trauma, and patients unwilling to participate were excluded from the study.

Method of patient evaluation: Clinical features

We evaluated the patients in terms of demographic details, age of onset of corneal opacity, family history, antenatal and birth history, systemic history, and past treatment history if any. Ocular examination was carried out under general anesthesia for young patients unco-operative for detailed examination and slit-lamp evaluation was done for cooperative children and adult patients. Laterality (unilateral or bilateral) was determined according to the presence of corneal opacities in these ASD disorders. The nature of corneal opacity (ground glass haze, leucomatous corneal opacity [LCO], etc.) was noted and limbal to limbal, horizontal, and vertical corneal diameters (CDs) were measured by Vernier calipers. The lens status was assessed during the examination of the anterior segment and was documented to be either clear or cataractous. For patients having dense corneal opacities wherein the lens status could not be visualized, ultrasound biomicroscopy (UBM) (35-MHz Vumax HD system, Sonomed Escalon, USA) was used to determine the lens status.

Clinical photographs were recorded for all patients with the Callisto Eye system integrated with the OPMI Lumera 700 microscope, Carl Zeiss AG, Germany. Posterior segment evaluation was done by indirect ophthalmoscopy in patients, wherein the size and density of the corneal opacity permitted posterior segment evaluation and optic disc findings (cup to disc ratio [CDR]) as well as any associated retinal findings were documented. B-scan ultrasonography (USG) for posterior segment evaluation and axial length using A-scan were done for all patients by Sonomed EZ Scan AB5500 + Ophthalmic Ultrasound Scanner, Sonomed Inc., Lake Success, NY, USA. Axial length was measured from the anterior corneal surface spike to the vitreoretinal interface spike. Intraocular pressure (IOP) was calculated by Perkins MK3 tonometer, Haag Streit, UK, for all patients. Best-corrected visual acuity was documented with suitable age-appropriate tests like the Cardiff acuity test at 50 cm/Snellen test.

16 eyes of 16 patients (7 eyes of 7 patients with CHED, 7 eyes of 7 patients with PA, and 2 eyes of 2 patients with PCG) underwent optical penetrating keratoplasty. Corneal button specimens for histopathological examination were obtained from the operation theater, fixed in 10% buffered formalin, embedded in paraffin blocks, and cut into 4 um thick sections. Sections were analyzed by light microscopy under low- (×10) and

high-power magnification (×25) after staining with hematoxylin and eosin stain.

Genetic evaluation was carried out in 23 patients (6 patients with CHED, 11 patients with PA, and 6 patients with PCG). A 5 ml sample of peripheral blood was collected by venipuncture in ethylenediaminetetraacetic acid vials from the patients after obtaining informed consent from all of the participants. Genomic data were extracted by the salting out method. The deoxyribonucleic acid (DNA) was checked for quality and quantity by the nano-spectrophotometer and processed for whole-exome sequencing (WES). The protocol followed for whole-exome enrichment was based on the Agilent SureSelect Human All Exon platform. The DNA was fragmented into 150–200 bp lengths followed by polymerase chain reaction (PCR) amplification and library preparation, capturing the hybrids on magnetic beads which were again amplified by PCR and the samples were processed for WES analysis. Variant calling was done using the wANNOVAR online annotation tool. The variants that were identified as mutations were further validated by PCR amplification using specific primers for the genes/mutation. The amplified PCR products were then subjected to gel purification using gel extraction kits (Qiagen GmBH) and the purified PCR products were screened for sequence changes by bidirectional sequencing. Nucleotide sequences for the coding regions were compared with the nucleotide sequence of the published gene sequences. Any change in nucleotide sequence was taken as a gene mutation. The significant mutations were then compared with the public database of gene mutations and classified as novel or reported mutations.

Method of patient evaluation: Imaging modalities

a. UBM was done with the 35 MHz Vumax HD system, Sonomed Escalon, USA. UBM examination was performed in the supine position after installation of topical anesthetic drops. The specially designed scleral cup was then fixed to the patient's eyes with 5% freshly prepared methyl cellulose gel being used as a coupling medium. UBM was performed with a 35 MHz transducer at the inferior limbus
   UBM parameters measured [Figure 1]:
   i. Central corneal thickness (CCT) was measured from the central inner surface of the corneal endothelium to the outer epithelial surface
   ii. Anterior chamber depth (ACD) was measured from the center of the corneal endothelium to the anterior lens capsule
   iii. Iris thickness (IT): IT was measured at the thickest region of the iris near the pupil
   iv. Ciliary body (CB) thickness: CB thickness was measured along the thickest dimension of the CB.

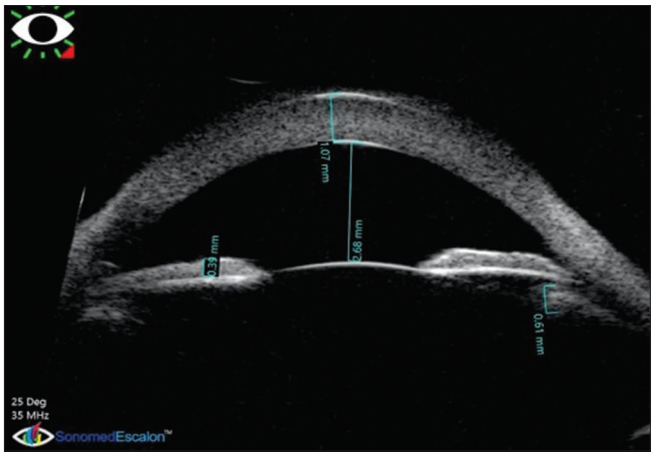

Figure 1: Methods for measurement of ultrasound biomicroscopy parameters

b. Microscope-integrated optical coherence tomography (i-OCT)-assisted imaging was done by Lumera 700 microscope and Rescan 700, Carl Zeiss AG, Germany, with OCT images projected on a separate screen. A standard cube size of 8mm was chosen to focus on corneal features in areas of opacity and specific characteristics were noted.

Statistical analysis

Statistical analysis was done using STATA 11.2 software for Windows and SPSS (version 12.1; Stata Corporation, College Station, Texas, USA). Descriptive statistics are shown and discussed as the mean and standard deviation for normally distributed variables and as the median and interquartile range for nonnormally distributed variables. Normally distributed patient characteristics were compared among all three groups using analysis of variance (ANOVA) and with *post-hoc* pairwise tests for ANOVA using the Tukey's HSD method for intergroup comparison. Data that were not normally distributed were compared among the three groups using the Kruskal–Wallis test. *Post-hoc* pairwise tests for the Kruskal–Wallis test were performed using the Dunn's test method with Sidak correction for intergroup comparison. Categorical variables were studied with Fisher's exact test with adjusted *P* values for intergroup comparison. $P < 0.05$ was considered statistically significant.

Results

Forty-two patients (74 eyes) were included in the analysis. In terms of demographic profile, the highest median age of presentation to the tertiary health-care center was seen in the CHED group, highlighting the later presentation of these patients to tertiary health-care centers as compared to PA and PCG patients. The age group of presentation for all three diseases was seen to lie in the amblyogenic period of visual development. In all the three groups of diseases, an almost equal male-to-

female ratio was noted in this study. The proportion of patients with positive family history and consanguinity was highest in the CHED group, while PA had the highest proportion of patients with a negative family history. Eventful antenatal history was seen in three patients with PA with 1 patient receiving rabies vaccine at 1.5 months of gestation, 1 patient having severe anemia in gestation, and 1 patient with a history of antenatal fever with a negative TORCH profile. There was no significant difference in terms of birth history and systemic associations in the patients of this study cohort [Table 1].

In the past treatment history, there was a significant difference between the three groups in terms of interventions for glaucoma (P = 0.01 using Fisher's exact test) as is highlighted in Table 2. Eight eyes of CHED were treated for glaucoma, of which 2 eyes underwent trabeculectomy and CHED was suspected, when the corneal haze did not clear post-IOP control in the postoperative period. One unilateral patient of PCG was lost to follow-up and underwent only initial medical management [Table 2].

Clinical characteristics

The distribution in terms of laterality and nystagmus association is highlighted in Table 1. 100% of patients with CHED presented with bilateral involvement, while unilateral involvement was seen in some patients with PA (44.44%) and PCG (15.38%) groups. Nystagmus was more common in CHED compared to the other two disorders. The various overlapping presentations of corneal opacities in the three disorders are well elucidated in Table 3 and Figure 2. All patients with CHED presented with diffuse ground glass haze, while central/paracentral leucomatous opacities were seen in patients with PA. Corneal opacities observed in PCG patients were in the form of diffuse haze, leucomatous opacities, or in the

Table 1: Demographic distribution and clinical history details among the three diseases

Parameter	Parameter	CHED (*n*=11 patients), *n* (%)	Peters (*n*=18 patients), *n* (%)	PCG (*n*=13 patients), *n* (%)	Adjusted intergroup (*P*)	*P*
Age of presentation	Mean±SD (months)	91.73±85.97	13.96±17.70	15.23±13.89	CHED and PA=0.001[d]	0.001[a,*]
	Median (IQR)	72 (48–9)	9 (2.25–21)	10 (3–24)	PA and PCG=0.938[d]	
	Range	1–288	0.3–72	1–48	CHED and PCG=0.015[d]	
Age of onset of corneal opacity	Since birth	11 (100)	14 (77.8)	11 (84.6)		0.539[b]
	<1 month	0	2 (11.1)	1 (7.7)		
	1–3 months	0	2 (11.1)	0		
	>3 months	0	0	1 (7.7)		
Gender	Male	6 (54.5)	9 (50.0)	6 (46.2)		0.920[c]
	Female	5 (45.5)	9 (50.0)	7 (53.8)		
Family history	Positive	6 (54.5)	0	2 (15.4)		<0.001[b,*]
	Negative	5 (45.5)	18 (100)	11 (84.6)		
Antenatal history	Normal	6 (54.5)	13 (72.2)	12 (92.3)		0.045[b,*]
	Consanguinity	5 (45.5)	2 (11.1)	1 (7.7)		
	Eventful antenatal period	0	3 (16.7)	0		
Birth history	FTNVD	9 (81.8)	13 (72.2)	8 (61.5)		0.526[b]
	FTLSCS	2 (18.2)	1 (5.6)	3 (23.1)		
	Eventful/preterm FTVD	0	3 (16.7)	2 (15.4)		
	Eventful/preterm LSCS	0	1 (5.6)	0		
Laterality	Unilateral	0	8 (44.44)	2 (15.38)		<0.014[b,*]
	Bilateral	11 (100)	10 (55.55)	11 (84.62)		
Nystagmus	Present	6 (54.5)	6 (33.3)	2 (15.4)		0.156[b]
	Absent	5 (45.5)	12 (66.7)	11 (84.6)		

[a]Kruskal–Wallis test, [b]Fisher's exact test, [c]Chi-squared test, [d]*Post-hoc* pairwise tests performed using Dunn's test with Sidak correction. FTNVD=Full term normal vaginal delivery, FTLSCS=Full term lower segment Cesarean section, FTVD=Full term vaginal delivery, LSCS=Lower segment Cesarean section, SD=Standard deviation, IQR=Interquartile range, PCG=Primary congenital glaucoma, CHED=Congenital hereditary endothelial dystrophy, PA=Peters anomaly. *P value<0.05

Table 2: Interventions for glaucoma across the three disease groups

	Glaucoma			No glaucoma
	Received medical treatment, *n* (%)	Trabeculectomy±medical treatment, *n* (%)	Total eyes receiving treatment for glaucoma, *n* (%)	
CHED (*n*=22 eyes)	6 (27.27)	2 (9.09)	8 (36.37)	14 (63.63)
Peters (*n*=28 eyes)	6 (22.72)	12 (42.8)	18 (64.28)	10 (35.72)
PCG (*n*=24 eyes)	24 (100)	23 (95.83)	24 (100)	0 (0.00)

Medical treatment characterized by 2 or more antiglaucoma medications. Trabeculectomy done using mitomycin C 0.2 mg/mL for 1–2 min. PCG=Primary congenital glaucoma, CHED=Congenital hereditary endothelial dystrophy

form of multiple Haab's striae. In terms of lens status, cataractous lenses were observed in 25% of PA patients, while all CHED and PCG patients had clear lenses [Table 3]. In PA eyes with cataractous lenses, Type 1 PA was seen in 5 eyes, whereas Type 2 PA was seen in 2 eyes.

In patients wherein posterior segment evaluation could be done with indirect ophthalmoscopy [Table 4], no retinal pathologies were found in any of the patients. The CHED group had the highest proportion of normal CDR, while the PCG group had the largest proportion of increased CDR in cases where fundoscopy could be done.

All patients underwent B-scan USG [Table 4], and there was a significant difference in the three groups. ONH cupping was present in 42.8% of the eyes of PA, highlighting the coexistence of glaucoma in PA. USG was found to be echoic in 3 eyes (1 unilateral and 1 bilateral) of PA with findings as follows:

1. Microphthalmos, vitreous hemorrhage, and increased chorioretinal thickening (1.3 mm) in a patient with unilateral PA
2. Vitreous hemorrhage with posterior vitreous detachment with absent cupping in the right eye of a patient with bilateral PA
3. Vitreous hemorrhage with anterior proliferative vitreoretinopathy with retinal detachment and absent cupping in the left eye of a patient with bilateral PA.

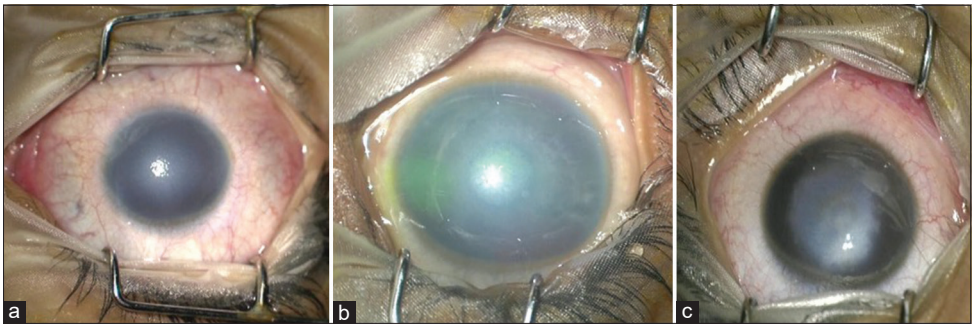

Figure 2: Similar clinical phenotypes seen in cases of congenital hereditary endothelial dystrophy (a), primary congenital glaucoma (b), and Peters anomaly (c)

Table 3: Nature of corneal opacity and lens status among the three disease groups

Parameter	CHED (*n*=22 eyes), *n* (%)	Peters (*n*=28 eyes), *n* (%)	PCG (*n*=24 eyes), *n* (%)	*P*
Nature of corneal opacity				
Diffuse corneal haze (limbus to limbus)	22 (100)	0	3 (12.5)	*P*<0.001[b,*]
Central/paracentral LCO	0	27 (96.4)	15 (62.5)	
Peripheral LCO with associated LSCD	0	1 (3.6)	0	
Multiple Haab's striae	0	0	6 (25)	
Lens status				
Clear	18	3	12	
Cataractous	0	0	0	
Not visible	4	25	12	

UBM finding for lens not visible	Clear on UBM (*n*=4)	Cataractous on UBM (*n*=0)	Clear on UBM (*n*=18)	Cataractous on UBM (*n*=7)	Clear on UBM (*n*=12)	Cataractous on UBM (*n*=0)	*P*
Total clear, *n* (%)	22 (100)		21 (75)		24 (100)		<0.05[b,*]
Total cataractous, *n* (%)	0		7 (25)		0		

[b]Fisher's exact test. LCO=Leucomatous corneal opacity, PCG=Primary congenital glaucoma, CHED=Congenital hereditary endothelial dystrophy, LSCD=Limbal stem cell deficiency, UBM=Ultrasound biomicroscopy. **P* value<0.05

Table 4: Posterior segment evaluation: Fundus findings and B-scan ultrasonography details

Parameter	Parameter: Posterior segment	CHED (*n*=22 eyes), *n* (%)	Peters (*n*=28 eyes), *n* (%)	PCG (*n*=24 eyes), *n* (%)	Total (*n*=74 eyes), *n* (%)	*P*
Funduscopy	Normal CDR	11 (50)	2 (7.1)	0	13 (17.6)	<0.001[b,*]
	Increased CDR	0	1 (3.6)	7 (29.2)	8 (10.8)	
	Poor glow	11 (50)	25 (89.3)	17 (70.8)	53 (71.6)	
Posterior segment B scan USG	Anechoic, cupping absent	22 (100)	13 (46.43)	0	35 (47.29)	<0.001[b,*]
	Anechoic, cupping present	0	12 (42.86)	24 (100)	36 (48.64)	
	Echoic for retinal detachment or vitreous hemorrhage, cupping absent	0	3 (10.71)	0	3 (4.05)	

[b]Fisher's exact test. CDR=Cup to disc ratio, USG=Ultrasonography, PCG=Primary congenital glaucoma, CHED=Congenital hereditary endothelial dystrophy. **P* value<0.05

There was a significant difference between the presenting visual acuities of the three groups with the CHED group having better baseline visual acuity (median LogMAR of 1.47) as compared to PA and PCG groups, respectively (adjusted $P < 0.001$ in intergroup comparison done by *post-hoc* pairwise tests for Kruskal–Wallis using Dunn's test with Sidak correction). The median VA of 2.7 LogMAR in both the groups of PA and PCG indicated a poor visual potential in these groups [Table 5]. The highest median IOP was found in the PCG group as compared to PA and CHED groups although not statistically significant [Table 5].

Investigations

There was a significant difference between the CDs in the three disease groups with the highest mean and median CDs in the PCG group. No significant difference was found in the comparison between CHED and PA groups, both showing normal age matched CDs [Table 6]. The axial length was found to be comparable in all the three disease groups [Table 7].

On UBM, increased central corneal thickness was seen in all disease groups. ACD was reduced in PA eyes as compared to CHED eyes which had a normal ACD and an increased ACD was seen in PCG eyes. IT and

Table 5: Visual acuity at presentation and intraocular pressure

Parameter	CHED (*n*=22 eyes)	Peters (*n*=28 eyes)	PCG (*n*=24 eyes)	*P*
Visual acuity				
Mean±SD	1.62±0.30	2.70±0.49	2.67±0.37	<0.001[a,*]
Median (IQR)	1.47 (1.47–1.77)	2.7 (2.7–3)	2.7 (2.7–3)	
Range	1.17–2.3	1–3	1.47–3	
IOP				
Mean±SD	16.91±5.61	18.93±10.45	23.21±8.87	0.038[a]
Median (IQR)	16 (13.25–20.75)	14 (12–26.5)	25 (17.5–28.25)	
Range	10–32	8–40	6–40	

[a]Kruskal–Wallis test. PCG=Primary congenital glaucoma, CHED=Congenital hereditary endothelial dystrophy, SD=Standard deviation, IQR=Interquartile range, IOP=Intraocular pressure. **P* value<0.05

Table 6: Comparison of corneal diameters across the three groups and between groups

Parameter: CD	CHED (*n*=22 eyes)	PA (*n*=28 eyes)	PCG (*n*=24 eyes)	Overall (*P*)	CHED - PCG (*P*)	CHED - PA (*P*)	PCG - PA (*P*)
CD (vertical), mean±SD	11.05±0.34	10.81±1.53	12.98±0.99	<0.001[a,*]	<0.001[d,*]	0.969[d]	<0.001[d,*]
CD (vertical), median (IQR)	11 (11–11.38)	11 (10–12)	13 (12.38–13.62)				
CD (horizontal), mean±SD	11.43±0.47	11.40±1.22	13.23±1.07	<0.001[a,*]	<0.001[d,*]	0.960[d]	<0.001[d,*]
CD (horizontal), median (IQR)	11.5 (11–11.88)	11.5 (10.5–12.38)	13 (12.5–14.12)				
CD (average), mean±SD	11.24±0.37	11.11±1.33	13.10±1.02	<0.001[a,*]	<0.001[d,*]	0.934[d]	<0.001[d,*]
CD (average), median (IQR)	11.25 (11–11.62)	11.25 (10.06–12.25)	12.88 (12.44–14)				

[a]Kruskal–Wallis test, [d]*Post-hoc* pairwise tests for Kruskal–Wallis test performed using Dunn's test method with Sidak correction. PCG=Primary congenital glaucoma, CHED=Congenital hereditary endothelial dystrophy, SD=Standard deviation, IQR=Interquartile range, PA=Peters anomaly, CD=Corneal diameter. **P* value<0.05

Table 7: Comparison of axial length between the three groups

Parameter: Axial length	CHED (*n*=22 eyes)	Peters (*n*=28 eyes)	PCG (*n*=24 eyes)	*P*
Mean±SD	22.26±2.09	21.09±3.05	21.68±4.20	0.532[e]
Median (IQR)	22.3 (20.79–23)	21.1 (19.18–23)	21.02 (20–25)	
Range	18.92–25.75	16–26.4	13–28	

[e]One-way ANOVA test. ANOVA=Analysis of variance, PCG=Primary congenital glaucoma, CHED=Congenital hereditary endothelial dystrophy, SD=Standard deviation, IQR=Interquartile range

Table 8: Comparison of ultrasound biomicroscopy parameters across the three groups and between groups

Parameter: UBM parameters	Mean±SD			Overall (*P*)	CHED - PCG (*P*)	CHED - Peters (*P*)	PCG - Peters (*P*)
	CHED	Peters	PCG				
CCT	1.04±0.09	1.12±0.36	0.96±0.33	0.263[e]	0.739[f]	0.729[f]	0.233[f]
ACD	2.66±0.23	1.54±0.70	3.40±1.01	<0.001[a,*]	0.209[d]	0.001[d,*]	<0.001[d,*]
IT	0.50±0.08	0.37±0.10	0.36±0.08	0.001[a,*]	<0.001[d,*]	0.003[d,*]	0.846[d]
CB thickness	0.73±0.15	0.56±0.23	0.50±0.07	0.003[a,*]	0.006[d,*]	0.007[d,*]	0.996[d]

**Post-hoc* pairwise tests for Kruskal–Wallis test performed using Dunn's test method with Sidak correction, [d]Kruskal–Wallis test, [e]One-way ANOVA test, [f]*Post-hoc* pairwise tests for ANOVA using Tukey's HSD method. CCT=Central corneal thickness, ACD=Anterior chamber depth, CB thickness=Ciliary body thickness, IT=Iris thickness, ANOVA=Analysis of variance, PCG=Primary congenital glaucoma, CHED=Congenital hereditary endothelial dystrophy, SD=Standard deviation, UBM=Ultrasound biomicroscopy

CB thickness were found to be significantly lesser in the PCG and PA groups compared to the CHED group [Table 8 and Figure 3].

UBM was also helpful in characterizing the type of PA. Type 1 PA was defined by the presence of central or paracentral leukoma with iridocorneal adhesions, Type 2 PA was defined by presence of a central or paracentral leukoma and kerato-lenticular contact with or without iridocorneal adhesions, while the third type of PA was characterized by the presence of only a posterior corneal defect and central leukoma without iridocorneal or kerato-lenticular adhesions. 60.71% (17 eyes) had Type 1 PA, 7.14% (2 eyes) had Type 2 PA, and 32.14% (9 eyes) had the third type of PA with only a posterior corneal defect with central leukoma [Figure 4]. One unilateral PCG patient with a LCO had an iris cyst which was identified on UBM.

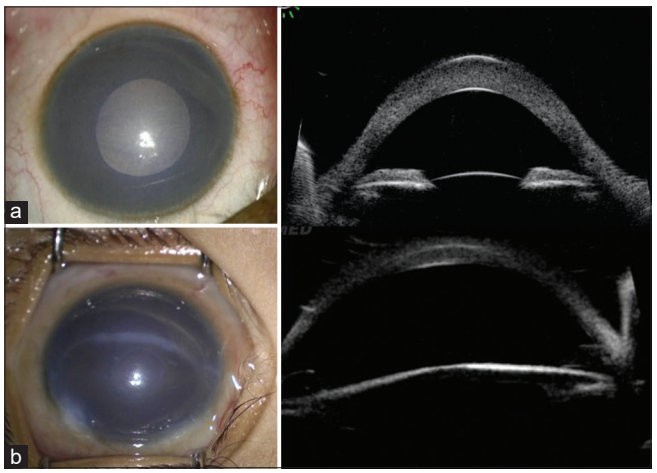

Figure 3: Anterior chamber details seen on ultrasound biomicroscopy in cases of congenital hereditary endothelial dystrophy (a) and primary congenital glaucoma eyes (b)

i-OCT was helpful in a noncontact, preoperative characterization of the type of corneal opacity. In CHED patients, diffuse hyperreflectivity was seen in the mid-stromal to deep-stromal levels with a smooth Descemet's membrane (DM). In PCG patients, mid-to-deep stromal hyperreflectivity with DM irregularities were seen in cases, where LCOs had developed following Haab's striae [Figure 5]. In PA, localized areas of stromal hyperreflectivity corresponding to the areas of corneal opacity as well as posterior corneal defects, iridocorneal, and kerato-irido-lenticular adhesions were identified and helped in classifying the subtype of PA [Figure 6].

Histopathological analysis was done and the characteristic histopathological features found in this study, common to each disease, are summarized in Table 9 and Figures 7, 8. Thickened Bowman's membrane and stromal edema was a common finding in all the three diseases. In CHED, spheroidal degeneration was seen in 2 cases aged 18 and 24 years, respectively.

Genetic evaluation was carried out in 23 patients [Table 10]. The identified genes and their mutations in the pathogenesis of the three diseases are enumerated in Table 10. SLC4A11 gene was the predominant gene in cases of CHED, while mutations in CYP1B1and CPAMD8 were seen in cases of PCG and mutations in FOXC1 and CYP1B1 were found in cases of PA. One novel mutation (c.1360_1361insGATG) was noted in CYP1B1 gene in a PCG patient.

In the distribution of mutations according to the type of PA, 80% (4 out of 5) of patients having the third type of PA with only a posterior corneal defect and central leukoma were found to have associated genetic mutations [Table 10]. Patients with Type 1 and Type 2

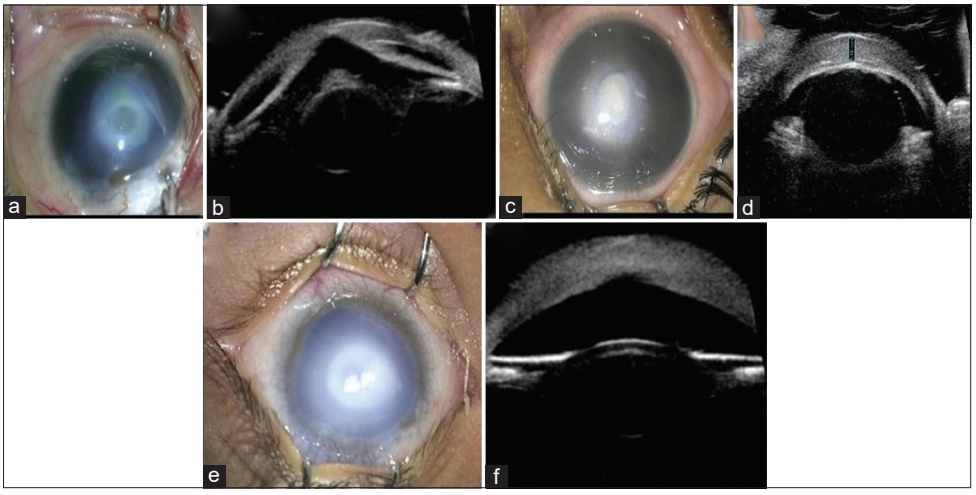

Figure 4: Types of Peters anomaly: Clinical picture and ultrasound biomicroscopy (UBM) of Type 1 Peters anomaly (PA) with iridocorneal adhesions (a and b); Clinical picture and UBM of Type 2 PA with kerato-irido-lenticular adhesions (c and d); Clinical picture and UBM of the third type of PA with only a central posterior corneal defect and no adhesions (e and f)

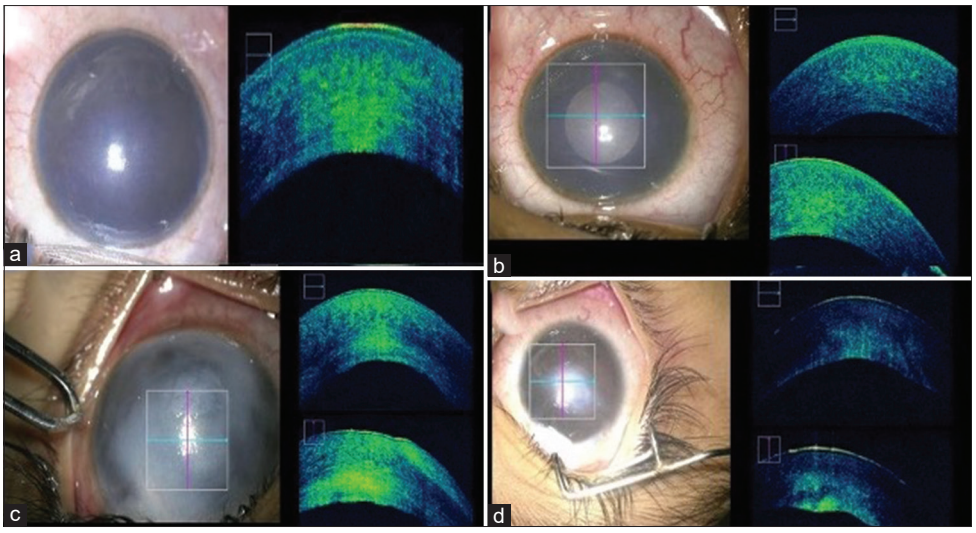

Figure 5: i-OCT based characterisation of corneal opacity in congenital hereditary endothelial dystrophy patients with diffuse stromal hyperreflectivity (a and b) and in primary congenital glaucoma patients with stromal hyperreflectivity and Descemet's membrane irregularities (c and d)

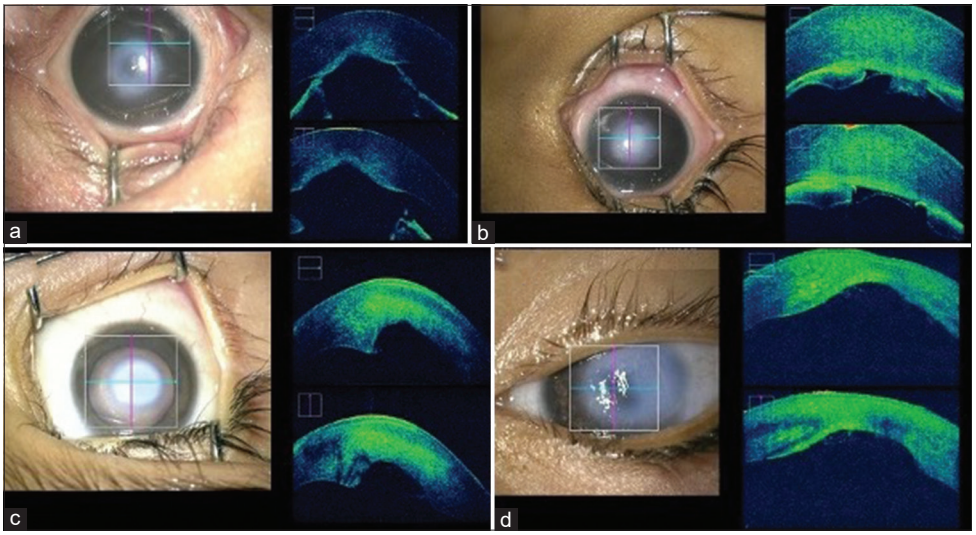

Figure 6: Intraoperative optical coherence tomography based characterization of corneal opacity in Peters Anomaly with Type 1 Peters anomaly (PA) (a) with a posterior corneal defect and iridocorneal adhesions, Type 2 PA (b) with keratoirido-lenticular adhesions, and Type 3 PA (c and d) with only a posterior corneal defect and no iridocorneal adhesions

Table 9: Characteristic histopathological features seen in the three disease groups

	Epithelium	Bowmans membrane	Stroma	DM	Endothelium
CHED	Edema present	Markedly thickened	Stromal edema (spheroidal degeneration in 2 cases)	Thickened	Atrophic endothelial cells Markedly reduced endothelial cell count
PA	Edema present	Thickened	Stromal edema	DM absent in center and present at periphery	Endothelium absent centrally and present peripherally
PCG	Mild edema present	Thickened	Stromal edema	Breaks in DM Thinned out DM	Decreased endothelial cell count

PCG=Primary congenital glaucoma, CHED=Congenital hereditary endothelial dystrophy, PA=Peters anomaly, DM=Descemet's membrane

PA were not found to have any associated genetic mutations.

The key differentiating features between the three disorders are summarized in Table 11.

Discussion

Congenital corneal disorders are an important cause of childhood blindness. ASD disorders are now known to occur due to developmental anomalies of the neural

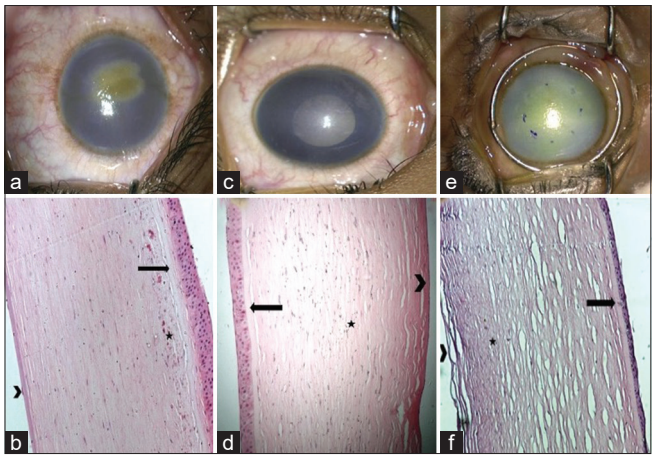

Figure 7: Histopathology specimens of corneal tissue of congenital hereditary endothelial dystrophy (CHED) patient 1 using H and E, stain ×10 magnification showing epithelial edema, thickened Bowman's membrane (black arrow), spheroidal degeneration (star) in the anterior part of stroma, stromal edema, thickened Descemet's membrane (DM) membrane with sparse endothelial cells (chevron) (a and b), CHED patient 2 using H and E, under ×10 magnification showing epithelial edema, thickened Bowman's membrane (black arrow), stromal edema (star), thickened DM membrane with sparse endothelial cells (chevron) (c and d) and primary congenital glaucoma patient using H and E, stain under ×10 magnification showing thickened Bowman's membrane (black arrow) and stromal edema (star) with DM thinning (chevron) (e and f)

crest cells or secondary mesenchyme. Nischal proposed a new classification of ASD disorders based on the type of developmental arrest, wherein they suggested that the late arrest of posterior migration of the iris resulted in congenital glaucoma, while the central cornea was affected due to late arrest in the final differentiation of the neural crest cells causing disorders like CHED, PA, PPCD, and ICE syndromes.[1]

Our study highlighted the clinical features of three ASD disorders presenting with infantile corneal opacities, namely, CHED, PA, and PCG.

The mean age of presentation for CHED and PCG patients was found to be similar to that seen by Sridhar *et al*. in CHED patients in South India (6.29 ± 1.92 years) and that reported by Senthil *et al*. with a mean age of 1.80 years (21.63 months) in PCG patients, respectively.[7,8] The age of presentation of PA was later as compared to that reported by Rao *et al*. (4.6 ± 2.5 months).[9] Despite manifesting at birth, patients with CHED presented significantly later to the tertiary health-care center as compared to patients with PCG and PA. This may be attributed to the slightly better visual acuity in CHED patients that still allow for day-to-day activities, therefore leading to a later presentation for seeking medical help.

The association of consanguinity and positive family history in CHED has been demonstrated in the literature as was documented in our study.[10,11] The majority of the cases of PA are found to have a sporadic inheritance, which is further evidenced by the findings

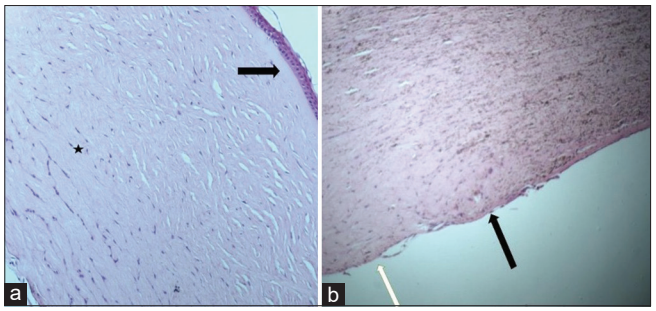

Figure 8: Histopathology specimen of corneal button of Peters Anomaly patient using H and E, under ×10 magnification showing thickened Bowman's membrane (arrow) and stromal edema (star) (a) and absence of Descemet's membrane (DM)-endothelium complex in the central part (white arrow) and presence of DM endothelial complex in the peripheral part (black arrow) (b)

in our study, wherein the PA group had the highest proportion of patients with no family history of the same disorder. However, cases of PA with autosomal recessive and dominant inheritance have been previously documented.[12,13] In a study by Tamçelik *et al*. in PCG patients, positive family history was noted in 21.2% of PCG patients, while consanguinity was noted in 53.2% of patients, a proportion much higher than that reported in our findings.[14]

Nystagmus was seen in 54.5% of CHED patients, which was similar to the incidence of nystagmus (55%) noted in the study conducted by Al-Rajhi and Wagoner.[15] The incidence of nystagmus in PA patients was 33.3% in our study, which was similar to the 32% incidence noted by Yang *et al*.,[16] while it was present in only 15.4% of PCG patients in our study as opposed to 22.1% cases of PCG in the study by Fang *et al*.[17] In all the three diseases, nystagmus may be present in the form of sensory nystagmus due to decreased visual feedback to the visual cortex due to dense corneal opacities.

In terms of laterality, our findings were in accordance with literature, in which cases of CHED presented with 100% bilaterality and in cases of PA and PCG, wherein the occurrence of bilaterality is reported to be much higher as compared to unilateral cases.[10,12,14]

Corneal opacities in the form of diffuse haze in CHED and PCG patients and pure leucomatous corneal opacities (LCO) seen in PA and PCG patients highlighted that all three diseases can present in the form of overlapping clinical features, making it difficult to accurately diagnose these diseases. Mullaney *et al*. confirmed that clinical characterization of neonatal corneal opacities in ASD disorders is a challenge due to the similar clinical manifestations and coexistence of diseases such as CHED and PA with congenital glaucoma.[18]

No systemic associations were found in PA patients. The proportion of Type 1 (60.71%) and Type 2 (7.14%)

Table 10: Distribution of genetic mutations in the 23 patients across disease groups

Disease	Gene mutations		
	CHED (*n*=6 patients), *n* (%)	PA (*n*=11 patients), *n* (%)	PCG (*n*=6 patients), *n* (%)
	Mutations present		
	6 (100)	4 (36.4)	5 (83.3)
	Gene	Mutation	Type of PA
CHED	SLC4A11	pR755Q,3214565<T splice variant	
CHED	SLC4A11	c.2606+1G>A	
CHED	SLC4A11	c.1979−2A>C	
CHED	SLC4A11	pR755Q	
CHED	SLC4A11	c.800G>A	
CHED	SLC4A11	3209483C.T splice variant	
PA	CYP1B1	c.1360_1361insGATG	Type 3 PA
PA	FOXC1	G(?_393153)_(1612107_?DEL)	Type 3 PA
PA	CYP1B1	c.1063C>T	Type 3 PA
PA	Chromosome 6:g.(?_393153_(3227543_?) del		Type 3 PA
PA	No mutation		Type 3 PA
PA	No mutation		Type 1 PA
PA	No mutation		Type 1 PA
PA	No mutation		Type 1 PA
PA	No mutation		Type 1 PA
PA	No mutation		Type 1 PA
PA	No mutation		Type 2 PA
PCG	CPAMD8	c.3563C>T	
PCG	CYP1B1	c.346_363del	
PCG	CYP1B1	c.1103G>A	
PCG	CYP1B1	c.349C>T	
PCG	CYP1B1	c.1360_1361insGATG*	
PCG	No mutation		

*Novel mutation SLC4A11, CYP1B1, FOXC1, CPAMD8. SLC4A11=Solute carrier family 4 member 11, CYP1B1=Cytochrome P450 family 1 subfamily B member 1, FOXC1=Forkhead box C1, CPAMD8=C3 and PZP-like alpha-2-macroglobulin domain-containing protein 8, PCG=Primary congenital glaucoma, CHED=Congenital hereditary endothelial dystrophy, PA=Peters anomaly

cases in our study were similar to that documented by Fouzdar-Jain *et al*. (71.5% Type 1 and 28.5% Type 2 in their study).[19] The third type of PA is the least documented in literature, while it was seen in 32.14% in our study cohort.[1] It is important to differentiate between the types of PA as Type 1 PA is associated with a good prognosis, while the visual prognosis remains poor for Type 2 PA.[19] Prognosis of the third type is not yet clearly documented in literature.

In our study, similar to that quoted by Asif *et al*. in CHED patients, 100% of eyes in the CHED group (22 eyes) had a clear crystalline lens.[20] In the review by Bhandari *et al*., 10 out of 58 (17.24%) cases of PA were associated with cataracts, of which only 2 patients (3.45%) had Type 2 PA. Type 2 PA with cataracts is very rare.[12,21] Similarly to our study, 33.33% of PA patients had cataractous lenses, of which only 2 patients had Type 2 PA. The presence of cataracts adds to the amblyogenic factors in such patients. Clear lenses were noted in 100% of eyes of the PCG group of our study.

In the study conducted by Yang *et al*., the mean preoperative visual acuity for the CHED group was 1.03 ± 0.25 logMAR, which was better than that observed in our study group.[22] In comparison to reported studies wherein the visual acuities seen in PA and PCG groups were 2.049 ± 0.965 and 0.37 ± 0.48 logMAR, respectively, the visual acuities were decreased in our study groups.[23,24]

A higher mean and median IOP was seen in the PCG group as compared to the CHED and PA groups though not statistically significant. Sihota *et al*. reported a mean IOP of 22.44 ± 9.5 mmHg in PCG patients similar to our study (23.21 ± 8.87 mmHg).[25] Jain *et al*. noted a mean IOP of 22.2 ± 7.1 mmHg in their review of 29 PA eyes at presentation, which was similar to our study (18.93 ± 10.45 mmHg).[19]

On B-scan USG, all eyes of CHED patients were anechoic and showed absent cupping. In patients with PA, 42.86% of PA eyes were anechoic and showed ONH cupping, while 10.71% (3 eyes) of PA showed vitreous hemorrhage (VH) without evidence of PHPV(Persistent Hyperplastic Primary Vitreous) stalk and one eye had an associated retinal detachment. Microphthalmia was seen in one of the PA eyes showing VH. This was in

Table 11: Summary table highlighting the differential features of congenital hereditary endothelial dystrophy, primary congenital glaucoma and peters anomaly

	CHED	PCG	PA
Age of onset	At birth	At birth or within the neonatal period	At birth or within the neonatal period
Gender	Male/female	Male/female	Male/female
Family history	May or may not be present	May or may not be present	Absent
Laterality	Bilateral	Unilateral/bilateral	Unilateral/bilateral
Associated symptoms	Nystagmus	Photophobia	Nystagmus
		Lacrimation	
		Blepharospasm	
Signs: Corneal features			
Clarity	Diffuse limbal to limbal ground glass corneal haze	Diffuse corneal haze/ leucomatous opacity	Central/paracentral LCO
CDs	Normal	Increased (>12 mm)	Normal
Corneal thickness	Increased	Increased	Increased
AC	Normal AC depth	Deep AC	Shallow AC
			Peters type 1: Iridocorneal adhesions extending from collarette to edge of posterior corneal defect
			Peter's type 2: Keratolenticular adhesions±iridocorneal adhesions
			Peters's type 3: Posterior corneal defect with no iridocorneal or kerato-lenticular adhesions
Lens	Clear	Clear	Clear/cataractous
Optic disc	Normal	Cupping+	Normal/cupping + (if coexisting glaucoma)
Posterior segment	Normal	Normal	Normal/VH/associated retinal detachment
Visual potential	Retain ambulatory vision	Poor visual potential	Poor visual potential
IOP	Normal	Raised(>21 mmhg)	Normal (increased if coexisting glaucoma)
Axial length	Normal	Normal/increased	Normal
UBM features			
CCT	Increased	Increased	Increased
ACD	Normal	Increased	Decreased
IT	Normal	Decreased thickness	Decreased thickness
CB thickness	Normal	Decreased thickness	Decreased thickness
i-OCT features			
Corneal stroma	Mid-to-deep stromal diffuse hyper reflectivity	Mid-to-deep stromal diffuse hyper reflectivity	Focal areas of deep stromal hyperreflectivity with defects in posterior corneal stroma
DM	Smooth DM	Irregular DM	Focal defects in DM with/without iridocorneal or kerato-irido-lenticular adhesions
Histopathology			
Epithelium	Diffuse epithelial edema	Diffuse epithelial edema	Epithelial edema present
Bowman's layer	Thickened Bowman's membrane	Thickened Bowman's membrane	Thickened Bowman's membrane
Stroma	Diffuse stromal edema	Diffuse stromal edema with stromal lamellae irregular and separated by fluid pockets	Stromal edema with central concave defect in posterior corneal stroma with disordered stromal lamellae
DM	Thickened DM	Breaks in DM with thinned out DM	Absence of DM in posterior central defect but normal DM in periphery
Endothelium	Atrophic endothelial cells with reduced count	Reduced endothelial count	Absence of endothelium centrally but normal endothelium in periphery
Genetic analysis			
Genes commonly involved	SLC4A11	CYP1B1, CPAMD8	CYP1B1, FOXC1

AC=Anterior chamber, IT=Iris thickness, CB=Ciliary body, DM=Descemet's membrane, SLC4A11=Solute carrier family 4 member 11, CYP1B1=Cytochrome P450 family 1 subfamily B member 1, FOXC1=Forkhead box C1, CPAMD8=C3 and PZP-like alpha-2-macroglobulin domain-containing protein 8, UBM=Ultrasound biomicroscopy, i-OCT=Intraoperative optical coherence tomography, CCT=Central corneal thickness, ACD=AC depth, IOP=Intraocular pressure, PCG=Primary congenital glaucoma, CHED=Congenital hereditary endothelial dystrophy, PA=Peters anomaly, CDs=Corneal diameters, LCO=Leucomatous corneal opacity, VH=Vitreous hemorrhage

contrast to the findings by Traboulsi and Maumenee, where microphthalmia or chorioretinal colobomas were seen in 25% of the eyes with a less common occurrence of RD and PHPV.[26]

Congenital glaucoma can be found to coexist with CHED and often the diagnosis of CHED is made when the corneal edema does not clear even after adequate IOP control.[18] Ramamurthy *et al*. described how such cases pose a diagnostic and therapeutic dilemma for the treating ophthalmologist.[27] In our study, 4 patients (36.37%) of CHED were apparently found to have increased IOPs (after adjusting for corneal thickness), in which corneal edema persisted despite IOP control by medical (3 patients) and surgical interventions (1 patient). Initial diagnosis of PCG was made in 2 of these patients. However, other signs of glaucoma were not noted such as buphthalmos or optic nerve head cupping. This supported the findings of Khan *et al*. who stated that IOPs may be falsely elevated in children with recessive CHED, leading to confusion with congenital glaucoma.[28]

Various studies have shown that 50%–70% of PA cases can be associated with glaucoma.[19] Similar to our study, 42.86% association with glaucoma was seen in PA patients, diagnosed with increased IOPs (after adjustment for corneal thickness) and presence of ONH cupping. 95.83% of the PCG eyes underwent trabeculectomy with trabeculotomy in our study.

There was no significant difference between the three groups in terms of axial length in our study and hence could not aid in differentiating the three disorders. Although ocular enlargement similar to that seen in uncomplicated axial myopia has been previously documented in CHED patients secondary to visual deprivation, the same was not observed in our study.[29] The mean axial length in the PA and PCG groups was found to be similar to the mean reported axial lengths of 21.76 ± 3.39 mm and 22.32 ± 2.60 mm, respectively.[30,31]

There was a significant difference in the horizontal, vertical, and average CDs between the CHED and PCG groups ($P < 0.001$) and between PCG and PA groups ($P < 0.001$), respectively. This is particularly helpful as overlapping features of corneal opacities often exist in these groups and CDs can be used as one of the factors for differentiation. The importance of normal CDs in CHED as a differentiating point from coexisting congenital glaucoma was highlighted by Kang *et al*. in their study.[32] Horizontal CDs documented in various studies for CHED, PA, and PCG were found to be similar to that reported in our study.[20,33-35] Thus, horizontal CD measurements can be a useful parameter to differentiate between the three diseases.

Histopathology in CHED was similar to that described by Paliwal *et al*. and Stainer *et al*. with a thickened Bowman's membrane, stromal edema, thickened DM, and atrophic and reduced endothelial cell count.[10,36-38] Spheroidal degeneration was present in 2 cases which corroborated with the findings mentioned by McCartney and Kirkness and Kumawat *et al*., wherein spheroidal degeneration was present in patients diagnosed with CHED.[39,40]

Histopathological features found in PA were similar to that described by Nischal *et al*. and Alkatan *et al*. with markedly thickened Bowman's membrane with stromal edema and absence of DM, endothelial complex centrally.[13,41] Histopathology in PCG patients demonstrated epithelial and stromal edema with a thickened Bowman's membrane and thinning of DM. This was in contrast to the findings by Al Shamrani *et al*., wherein Bowman's membrane was found to be absent or fragmented and stromal scarring was present.[42]

Mutations in the SLC4A11 (sodium borate cotransporter) gene were found in all the CHED cases that underwent testing (6 patients). It was interesting to note that 5 out of the 6 patients in our study group did not have any history of consanguinity. In the study carried out by Sultana *et al*., 2 out of 8 families were found to be non-consanguineous, thus showing that consanguinity was not present in all patients with autosomal recessive CHED.[43] In PCG, mutations were identified in 83.3% (5/6) of cases in our study group. Mutation in the CPAMD8 gene was identified in one patient and in the CYP1B1 gene in the rest of the patients. CYP1B1 gene mutations on locus GLC3A have a strong association with PCG as is evidenced by literature, which was similar to the findings of our study.[44,45]

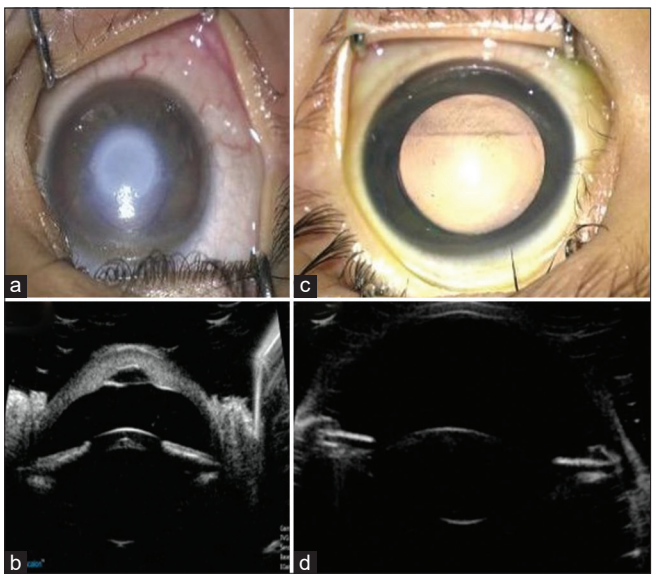

Figure 9: Patient phenotype with novel CYP1B1 mutation. PA phenotype in right eye of the patient, characterized by central leucomatous corneal opacity with normal corneal diameters and ultrasound biomicroscopy (UBM) findings of only a posterior corneal defect with no iridocorneal adhesions corresponding to Type 3 PA subtype (a and b) and primary congenital glaucoma (PCG) phenotype characterized by increased corneal diameters with mild haze in left eye and UBM suggestive of increased anterior chamber depth seen in PCG eyes(c and d)

One novel mutation in CYP1B1 was noted for the first time in our study causing an amino acid substitution (p. Lys454ArgfsTer2). This patient had features suggestive of the third type of PA in one eye and that suggestive of PCG in the other eye, highlighting the overlap both phenotypically and genetically between the two disorders [Figure 9]. CPAMD8 mutations are found to be associated with ASD disorders. These mutations are the second most common inherited cause of childhood glaucomas after CYP1B1. It was seen that most of the patients with CPAMD8 mutations revealed some abnormalities in the anterior segment structure such as iris hypoplasia, corectopia, and ectopia lentis.[46] This was, however, found to be absent in our case with this mutation [Figure 10]. Siggs *et al*. suggested that aqueous outflow dysfunction could be causative in the development of glaucoma in such cases. Thus, we found that in our study, patients with CPAMD8 mutations can present with PCG even in the absence of obvious anterior segment anomalies and possibly secondary to aqueous outflow dysfunction, further suggesting the overlap between congenital glaucoma and ASD disorders.[46,47]

Although most of the PA cases are thought to occur sporadically, they can be associated with mutations or deletions of homeobox genes involved in the development of the anterior segment.[12] Our study highlighted the fact that the sporadic occurrence of inheritance was seen in the majority of PA cases. Mutations were seen in CYP1B1 and FOXC1 gene, which was found to be consistent with the genes associated with PA as mentioned by Bhandari *et al*.[12] One case showed a unique mutation on a gene present on chromosome 6 (chr6:g.?_393153_[3227543_?] del). We found that no mutations were detected in the patients with Type 1 and Type 2 PA. However, interestingly, the third type of PA with only a posterior corneal defect was associated with 80% of the mutations (4 / 5 patients). Further studies can be undertaken to look for the genetic association in this PA type. This is especially important to provide genetic counseling to parents planning subsequent pregnancies in children with PA.

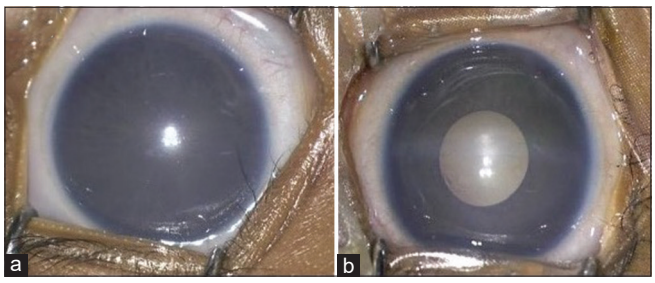

Figure 10: Phenotype in a patient with CPAMD8 mutation. Clinical image of the left eye characterized by diffuse corneal haze with a normal anterior segment (a) and clinical image of the right eye of the same patient characterized by diffuse corneal haze with prominent Haab's striae but normal anterior segment (b)

The role of UBM in diagnosing conditions with CCO was highlighted by Nischal *et al*.[41] UBM was useful in delineating the entire details of the anterior segment in eyes with corneal opacities, subclassifying that the types of PA and UBM parameters such as ACD, IT and CB thickness could be useful to differentiate between the three diseases. ACD (3.40 ± 1.01) and IT (0.36 ± 0.08) in PCG eyes were found to be similar to that documented by Hussein *et al*. (3.55 ± 0.32 mm and 0.38 ± 0.08mm), while CB thickness (0.50 ± 0.07mm) was found to be slightly lesser than that reported by Gupta *et al*. (0.80 ± 0.30mm).[33,35] One of the drawbacks of UBM was that it did not delineate the corneal characteristics in eyes with corneal opacities due to its lower resolution. It was also a contact procedure that was slightly cumbersome to carry out especially intraoperatively.

These drawbacks of UBM could be overcome with the use of i-OCT. The use of i-OCT in screening pediatric corneal opacities in order to facilitate dynamic visualization of the entire anterior segment was shown by Siebelman *et al*.[48] Sharma *et al*. found that i-OCT had a higher ability than UBM in delineating anterior segment details due to its higher resolution and magnification compared to UBM and is a useful noncontact tool in diagnosing pediatric corneal opacities as the examination of these patients has to be done largely under general anesthesia.[49] In our study, i-OCT was helpful in highlighting structural corneal details in terms of type (diffuse/localized) and extent of opacity (mid stromal/deep stromal), assessing the contour of DM (smooth/irregular) and identifying subtle posterior corneal defects/iridocorneal or kerat-irido-lenticular adhesions in PA, thereby helping in the diagnosis. It does, however, have its own drawbacks in terms of cost, restriction of scanning zone and distortion during eye movements.

Conclusion

The burden of disease in ASD disorders is due to corneal opacities, glaucoma, and cataracts which have their implications in the development of dense amblyopia in infancy contributing to blindness in these children.[6] This study, thus, highlights the distinctive clinical features including genetics and histopathological characteristics of three ASD disorders of CHED, PA, and PCG that can aid in the diagnosis of these diseases and can guide the appropriate interventions to be carried out as per the disease etiology. Furthermore, detailed genetic analysis can be carried out in patients with PA to find genetic associations, especially in the rare third subtype of PA and can aid in genetic counseling. In cases of phenotypic overlap, imaging modalities such as UBM and i-OCT can be used to differentiate between these disorders in terms of both quantitative and qualitative parameters and thus aid in the clinical diagnosis of these disorders.

Data availability statement

All data generated or analyzed during this study are included in this published article [and its supplementary information files].

Financial support and sponsorship

Nil.

Conflicts of interest

The authors declare that there are no conflicts of interests of this paper.

References

1. Nischal KK. Developmental anomalies of the anterior segment and globe. In: Wright KW, Spiegel PH, editors. Pediatric Ophthalmology and Strabismus. New York, NY:Springer New York; 2003. p. 369-90. Available from: https://www.researchgate.net/publication/300394392_Developmental_Anomalies_of_the_Anterior_Segment_and_Globe. [Last accessed on 2020 Apr 11].
2. Stahl ED. Anterior segment dysgenesis. Int Ophthalmol Clin 2014;54:95-104.
3. Idrees F, Vaideanu D, Fraser SG, Sowden JC, Khaw PT. A review of anterior segment dysgeneses. Surv Ophthalmol 2006;51:213-31.
4. Shigeyasu C, Yamada M, Mizuno Y, Yokoi T, Nishina S, Azuma N. Clinical features of anterior segment dysgenesis associated with congenital corneal opacities. Cornea 2012;31:293-8.
5. Ma AS, Grigg JR, Jamieson RV. Phenotype-genotype correlations and emerging pathways in ocular anterior segment dysgenesis. Hum Genet 2019;138:899-915.
6. Rezende RA, Uchoa UB, Uchoa R, Rapuano CJ, Laibson PR, Cohen EJ. Congenital corneal opacities in a cornea referral practice. Cornea 2004;23:565-70.
7. Sridhar S, Kumar K, Preethi B, Mittal P, Gangasagara SB. Demography of corneal dystrophies at a tertiary eye care centre in South India. IJCEO 2020;6:576-80.
8. Senthil S, Badakere S, Ganesh J, Krishnamurthy R, Dikshit S, Choudhari N, *et al.* Profile of childhood glaucoma at a tertiary center in South India. Indian J Ophthalmol 2019;67:358-65.
9. Rao KV, Fernandes M, Gangopadhyay N, Vemuganti GK, Krishnaiah S, Sangwan VS. Outcome of penetrating keratoplasty for Peters anomaly. Cornea 2008;27:749-53.
10. Paliwal P, Sharma A, Tandon R, Sharma N, Titiyal JS, Sen S, *et al.* Congenital hereditary endothelial dystrophy – Mutation analysis of SLC4A11 and genotype-phenotype correlation in a North Indian patient cohort. Mol Vis 2010;16:2955-63.
11. Firasat S, Dur-E-Shawar, Khan WA, Sughra U, Nousheen, Kaul H, *et al.* SLC4A11 mutations causative of congenital hereditary endothelial dystrophy (CHED) progressing to Harboyan syndrome in consanguineous Pakistani families. Mol Biol Rep 2021;48:7467-76.
12. Bhandari R, Ferri S, Whittaker B, Liu M, Lazzaro DR. Peters anomaly: Review of the literature. Cornea 2011;30:939-44.
13. Alkatan HM, Al Dhaheri H, Al Harby M. Terminology of Peters' anomaly variants: Summary of histopathological findings in 6 corneas and detailed clinicopathological correlation in 2 cases. Saudi J Ophthalmol 2019;33:277-82.
14. Tamçelik N, Atalay E, Bolukbasi S, Çapar O, Ozkok A. Demographic features of subjects with congenital glaucoma. Indian J Ophthalmol 2014;62:565-9.
15. Al-Rajhi AA, Wagoner MD. Penetrating keratoplasty in congenital hereditary endothelial dystrophy. Ophthalmology 1997;104:956-61.
16. Yang LL, Lambert SR, Lynn MJ, Stulting RD. Surgical management of glaucoma in infants and children with Peters' anomaly: Long-term structural and functional outcome. Ophthalmology 2004;111:112-7.
17. Fang L, Hu Y, Zhong Y, Xiao H, Lin S, Zhu Y, *et al.* Long-term visual outcomes of primary congenital glaucoma in China. Ophthalmic Res 2022;65:342-50.
18. Mullaney PB, Risco JM, Teichmann K, Millar L. Congenital hereditary endothelial dystrophy associated with glaucoma. Ophthalmology 1995;102:186-92.
19. Fouzdar-Jain S, Ibrahim Z, Reitinger J, Cao D, Mocan MC. Visual outcomes in pediatric patients with Peters anomaly. Clin Ophthalmol 2021;15:2591-6.
20. Asif MI, Bafna RK, Sharma N, Kaginalkar A, Sinha R, Agarwal T, *et al.* Microscope integrated optical coherence tomography guided descemet stripping automated endothelial keratoplasty in congenital hereditary endothelial dystrophy. Clin Ophthalmol 2021;15:3173-81.
21. Medsinge A, Nischal KK. Cataract surgery in children with congenital keratolenticular adhesion (Peters anomaly type 2). J AAPOS 2015;19:24-8.
22. Yang F, Hong J, Xiao G, Feng Y, Peng R, Wang M, *et al.* Descemet stripping endothelial keratoplasty in pediatric patients with congenital hereditary endothelial dystrophy. Am J Ophthalmol 2020;209:132-40.
23. Chang JW, Kim JH, Kim SJ, Yu YS. Long-term clinical course and visual outcome associated with Peters' anomaly. Eye (Lond) 2012;26:1237-42.
24. Esfandiari H, Prager A, Hassanpour K, Kurup SP, Mets-Halgrimson R, Yoon H, *et al.* The long-term visual outcomes of primary congenital glaucoma. J Ophthalmic Vis Res 2020;15:326-30.
25. Sihota R, Sidhu T, Agarwal R, Sharma A, Gupta A, Sethi A, *et al.* Evaluating target intraocular pressures in primary congenital glaucoma. Indian J Ophthalmol 2021;69:2082-7.
26. Traboulsi EI, Maumenee IH. Peters' anomaly and associated congenital malformations. Arch Ophthalmol 1992;110:1739-42.
27. Ramamurthy B, Sachdeva V, Mandal AK, Vemuganti GK, Garg P, Sangwan VS. Coexistent congenital hereditary endothelial dystrophy and congenital glaucoma. Cornea 2007;26:647-9.
28. Khan AO, Al-Shehah A, Ghadhfan FE. High measured intraocular pressure in children with recessive congenital hereditary endothelial dystrophy. J Pediatr Ophthalmol Strabismus 2010;47:29-33.
29. Twomey JM, Gilvarry A, Restori M, Kirkness CM, Moore AT, Holden AL. Ocular enlargement following infantile corneal opacification. Eye (Lond) 1990;4 (Pt 3):497-503.
30. Nassim S, Calixto AD. Peters anomaly: A clinical study of 36 patients. Invest Ophthalmol Vis Sci 2015;56:5640.
31. Al-Obaida I, Al Owaifeer AM, Ahmad K, Malik R. The relationship between axial length, age and intraocular pressure in children with primary congenital glaucoma. Sci Rep 2020;10:17821.
32. Kang BS, Jeoung JW, Oh JY. Inaccuracy of intraocular pressure measurement in congenital corneal opacity: Three case reports. BMC Ophthalmol 2020;20:3.
33. Hussein TR, Shalaby SM, Elbakary MA, Elseht RM, Gad RE. Ultrasound biomicroscopy as a diagnostic tool in infants with primary congenital glaucoma. Clin Ophthalmol 2014;8:1725-30.
34. Yoshikawa H, Sotozono C, Ikeda Y, Mori K, Ueno M, Kinoshita S. Long-term clinical course in eyes with Peters anomaly. Cornea 2017;36:448-51.
35. Gupta V, Jha R, Srinivasan G, Dada T, Sihota R. Ultrasound biomicroscopic characteristics of the anterior segment in primary congenital glaucoma. J AAPOS 2007;11:546-50.
36. Pearce WG, Tripathi RC, Morgan G. Congenital endothelial

corneal dystrophy. Clinical, pathological, and genetic study. Br J Ophthalmol 1969;53:577-91.
37. Ehlers N, Módis L, Møller-Pedersen T. A morphological and functional study of congenital hereditary endothelial dystrophy. Acta Ophthalmol Scand 1998;76:314-8.
38. Stainer GA, Akers PH, Binder PS, Zavala EY. Correlative microscopy and tissue culture of congenital hereditary endothelial dystrophy. Am J Ophthalmol 1982;93:456-65.
39. Kumawat BL, Gupta R, Sharma A, Sen S, Gupta S, Tandon R. Delayed onset of congenital hereditary endothelial dystrophy due to compound heterozygous SLC4A11 mutations. Indian J Ophthalmol 2016;64:492-5.
40. McCartney AC, Kirkness CM. Comparison between posterior polymorphous dystrophy and congenital hereditary endothelial dystrophy of the cornea. Eye (Lond) 1988;2 (Pt 1):63-70.
41. Nischal KK, Naor J, Jay V, MacKeen LD, Rootman DS. Clinicopathological correlation of congenital corneal opacification using ultrasound biomicroscopy. Br J Ophthalmol 2002;86:62-9.
42. Al Shamrani M, Al Hati K, Alkatan H, Alharby M, Jastaneiah S, Song J, *et al.* Pathological and immunohistochemical alterations of the cornea in congenital corneal opacification secondary to primary congenital glaucoma and peters anomaly. Cornea 2016;35:226-33.
43. Sultana A, Garg P, Ramamurthy B, Vemuganti GK, Kannabiran C. Mutational spectrum of the SLC4A11 gene in autosomal recessive congenital hereditary endothelial dystrophy. Mol Vis 2007;13:1327-32.
44. Khan AO. Genetics of primary glaucoma. Curr Opin Ophthalmol 2011;22:347-55.
45. Ling C, Zhang D, Zhang J, Sun H, Du Q, Li X. Updates on the molecular genetics of primary congenital glaucoma (Review). Exp Ther Med 2020;20:968-77.
46. Siggs OM, Souzeau E, Taranath DA, Zhou T, Dubowsky A, Javadiyan S, *et al*. Congenital glaucoma with anterior segment dysgenesis in individuals with biallelic CPAMD8 variants. bioRxiv. 2018 Apr 9:297077. Available from: https://www.biorxiv.org/content/10.1101/297077v1.full. [Last accessed on 2022 Jun 13].
47. Siggs OM, Souzeau E, Taranath DA, Dubowsky A, Chappell A, Zhou T, *et al.* Biallelic CPAMD8 variants are a frequent cause of childhood and juvenile open-angle glaucoma. Ophthalmology 2020;127:758-66.
48. Siebelmann S, Hermann M, Dietlein T, Bachmann B, Steven P, Cursiefen C. Intraoperative optical coherence tomography in children with anterior segment anomalies. Ophthalmology 2015;122:2582-4.
49. Sharma N, Priyadarshini K, Agarwal R, Bafna RK, Nagpal R, Sinha R, *et al*. Role of microscope-intraoperative optical coherence tomography in pediatric keratoplasty: A comparative study. Am J Ophthalmol 2021;221:190-8.